https://doi.org/10.37434/tpwj2021.08.08

MATHEMATICAL MODELING OF HYDRODYNAMIC AND THERMAL PROCESSES AT CRYSTALLIZATION OF TITANIUM INGOTS PRODUCED BY EBM

S.V. Akhonin[1], **V.O. Berezos**[1], **O.I. Bondar**[2], **O.I. Glukhenkyi**[2], **Yu.M. Goryslavets**[2] and **A.Yu. Severin**[1]
[1]E.O. Paton Electric Welding Institute of the NAS of Ukraine
11 Kazymyr Malevych Str., 03150, Kyiv, Ukraine. E-mail: office@paton.kiev.ua
[2]Institute of Electrodynamics of the NAS of Ukraine
56 Peremohy Prosp., 03057, Kyiv, Ukraine. E-mail: bondar_o_i@ukr.net

It is shown that when specifying the efficiency of EBM process, the phenomenon of thermogravitational convection is a weighty factor, which determines the thermal state of the ingot. A mathematical model of interrelated hydrodynamic and thermal processes in the crystallizing metal, taking into account the phenomena of thermogravitational convection, was formulated for a steady-state mode of the process of electron beam melting of titanium into a straight-through cylindrical mould. The thermal state of the ingot as well as the position of the crystallization front at a continuous feeding of liquid titanium from the cold hearth into the mould depending on metal temperature at the inlet and speed of ingot drawing for a laminar mode of hydrodynamic flow in the liquid pool was determined. It is found that at increase of metal temperature at the inlet into the mould in the studied range (2040–2100 K) shifting of the point of maximum pool depth from the ingot axis becomes smaller. Calculations within the constructed mathematical model were used to study the impact of the rate of liquid metal feed from the cold hearth into the mould on the shape and depth of a liquid pool. It is found that at increase of ingot drawing rate by 30 % the liquid pool depth increases by 1.5 times, and the point of the maximum liquid pool depth becomes close to the ingot axis. 10 Ref., 1 Table, 9 Figures.

Keywords: mathematical modeling; electron beam melting; hydrodynamic and thermal processes; ingot; titanium; continuous casting

Solidification of metal in the mould during electron beam melting (EBM) is accompanied by complex and transient physical processes of heat transfer, hydrodynamic flows and radiation. In practice, it is often impossible to measure values of the parameters in these processes, especially with a sufficient accuracy. In addition, in metallurgy, full-scale experiments are labour-consuming and involve high material costs because of a high energy consumption and cost of a melted metal. Therefore, numerical experiments with the use of methods of mathematical modeling and calculations in computers are of great importance, which allow making a qualitative and quantitative picture of the phenomena occurring in metallurgical processes at relatively low costs and a minimal amount of experimental data.

In [1, 2] the basic principles of modeling thermophysical processes in ingots produced by the methods of special electrometallurgy are formulated. Regarding the processes describing different stages of EBM, such as melting of the initial charge, mixing and evaporation of metal and impurities in the cold hearth, ingot formation in the mould, ingot cooling etc., they were considered in [3–6]. However, in the mentioned works, taking into account the complexity of solving interrelated three-dimensional multiphysical problems and the limited available calculating resources, a mathematical modeling of thermophysical processes in producing titanium ingots was mainly reduced to considering the thermal state of the ingot without heat and mass transfer due to the movement of a melt in the mould.

The modern development of numerical methods and ever-increasing capacity of computer technologies provide a possibility of formulating more complete and complex problems of modeling technological processes and the numerical approach is the most attractive in the study of hydrodynamic processes and processes of heat and mass transfer that occur while producing ingots by EBM method. In [7], a three-dimensional mathematical model of interrelated hydrodynamic and thermal processes of metal solidification in a straight-through cylindrical mould during electron beam melting with a cold hearth was presented and considered in detail. This mathematical model allows studying the processes in the quasi-fatigue mode of continuous ingot melting, during which the position of the crystallization front of the alloy in the mould does not change over time. On the example of the ingot of titanium Ti–6Al–4V alloy, which solidi-

S.V. Akhonin — https://orcid.org/0000-0002-7746-2946, V.O. Berezos — https://orcid.org/0000-0002-5026-7366,
O.I. Bondar — https://orcid.org/0000-0002-1678-8862, O.I. Glukhenkyi — https://orcid.org/0000-0001-5053-5677,
Yu.M. Goryslavets — https://orcid.org/0000-0003-1668-4972, A.Yu. Severin — https://orcid.org/0000-0003-4768-2363

fies in a cylindrical mould with a diameter of 0.6 m, it was shown that the effect of a turbulent thermal conductivity on the position of the crystallization front and the liquid pool depth is negligible for a set speed of ingot drawing (4 mm/min). In this case this allows making assumptions about the presence of turbulence only in the zone of inlet of the liquid metal jet from the cold hearth into the mould and about the predominant laminar nature of a melt in the liquid pool in general.

The shape and depth of a liquid pool can be more significantly affected by the overheating temperature of the liquid metal fed from the cold hearth and the efficiency of the continuous casting process. Therefore, the aim of this study is to determine the thermal state of the ingot and the position of the crystallization front at a continuous feeding of liquid titanium from the cold hearth into the mould depending on the metal temperature at the inlet and the speed of ingot drawing for a laminar hydrodynamic flows in the liquid pool. The study of these issues was carried out on the example of casting commercial titanium into a straight-through cylindrical mould of 0.4 m diameter.

For modeling the metnioned process, the following mathematical model was formulated, which includes the laws of conservation of mass (1), pulse (2) and power (3):

$$\nabla(\rho\mathbf{u}) = 0; \tag{1}$$

$$\rho(\mathbf{u}\cdot\nabla)\mathbf{u} = -\nabla p + \nabla\cdot\left(\mu\left(\nabla\mathbf{u} + (\nabla\mathbf{u})^T\right) - \right. \tag{2}$$

$$\left. -\frac{2}{3}\mu(\nabla\cdot\mathbf{u})\mathbf{I}\right) + \rho\mathbf{g} + \frac{C(1-F_L)^2}{q+F_L^3}(\mathbf{u}-\mathbf{u}_{\text{cast}});$$

$$\rho C_p(\mathbf{u}\cdot\nabla)T = -(\nabla\cdot\mathbf{q}), \tag{3}$$

where ρ is the density; **u** is the speed; p is the pressure; μ is the dynamic viscosity; **I** is a single matrix; **g** is the gravity vector; $C = 10^5$ and $q = 0.01$ are the constants, the ratio of which should be sufficient to suppress the movement (except for the casting speed $\mathbf{u}_{\text{cast}}$) in the solid zone; F_L is the fraction of the liquid phase (varies in the range from 0 to 1); $\mathbf{u}_{\text{cast}}$ is the vector of speed of ingot drawing; C_p is the specific heat capacity; T is the temperature; $\mathbf{q} = -k\nabla T$ is the heat flux due to thermal conductivity; k is the coefficient of thermal conductivity.

The position of the crystallization front was determined in accordance with the phase field method. The essence of the method consists in the fact that the phase transition occurs in a certain temperature range of $\Delta T = T_l - T_s$. The liquid zone is determined by the temperature higher than the liquidus temperature T_l, the solid zone is the temperature lower than the solidus temperature T_s, and the transition zone is between

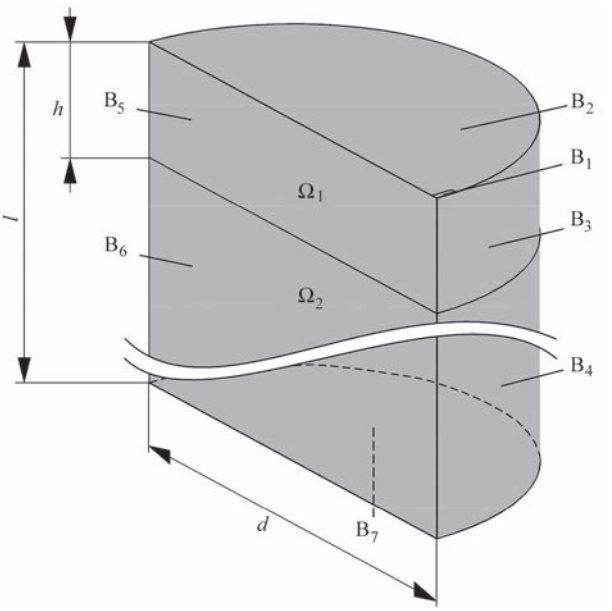

Figure 1. Calculation region for numerical modeling

them. The crystallization front is determined by the isotherm of melting temperature $T_m = T_s + \Delta T/2$. Expressions for determination of the fraction of a liquid phase F_l and the corresponding physical properties of materials in the transition zone (zone of phase state variation) are presented in [7].

The calculation region for studying the mentioned processes is presented in Figure 1, where B_1–B_7 are the borders of the calcualtion region, d = 0.4 m, h = = 0.15 m, $l = 2{\cdot}d$, the intersection of a melt jet at the inlet into the mould (**B**$_1$) is 10×40 mm.

The boundary conditions for the calculation region presented in Figure 1 are given in theTable, where **n** is the vector of normal to the surface; u_{cast} is the speed of ingot drawing; q_{ev} is the thermal flux from the surface of liquid metal due to evaporation; ε is the radiation coefficient; h is the coefficient of contact heat dissipation; $\sigma_{SB} = 5.67{\cdot}10^{-8}$ W/t(m$^2{\cdot}$K$_4$) is the Stefan–Boltzman constant; T_{amb} = 293.15 K is the ambient temperature.

Physical characteristics of titanium are as follows: melting temperature T_m = 1941 K; latent melting heat L = 295 kJ/kg; coefficient of dynamic viscosity for the liquid zone μ_l = 0.0035 Pa·s; coefficient of dynamic viscosity for the solid zone μ_s = 1 Pa·s. Therefore, at a set temperature range of the phase transition ΔT = = 60 K, liquidus temperature was T_l = 1971 K and solidus temperature was T_s = 1911 K. Characteristics of the transition zone (phase transition zone) were determined according to the method of total heat capacity (apparent heat capacity formulation).

Temperature dependences of the specific heat capacity $C_p(T)$, coefficient of thermal conductivity $k(T)$ and density $\rho(T)$ for solid and liquid phases of titanium are presented in Figure 2, *a*–*c* respectively [8]. The depen-

Boundary conditions of calculation region for numerical modelling

Boundary	Conditions for speed	Conditions for heat flux
B_1	$\mathbf{u} - (\mathbf{u}\cdot\mathbf{n})\mathbf{n} = 0$	$T = T_{in}$
B_2	$\mathbf{u}\cdot\mathbf{n} = 0$ $\mathbf{K} - (\mathbf{K}\cdot\mathbf{n})\mathbf{n} = 0$ $\mathbf{K} = \mu\left(\nabla\mathbf{u} + (\nabla\mathbf{u})^T\right)\mathbf{n}$	$-\mathbf{n}\cdot\mathbf{q} = \varepsilon_2\sigma\left(T_{amb}{}^4 - T^4\right) - q_{ev} + \frac{3P_{eb}}{\pi d^2}$ $\varepsilon_2 = 0.5$
B_3		$-\mathbf{n}\cdot\mathbf{q} = \varepsilon_3\sigma\left(T_{amb}{}^4 - T^4\right) + h_3\left(T_{amb} - T\right)$ $\varepsilon_3 = 0.35\left(1 - F_l\right)$ $h_3 = h_s\left(1 - F_l\right) + h_l F_l$ $h_s = 60$ W/(m²·K) $h_l = 2000$ W/(m²·K)
B_4		$-\mathbf{n}\cdot\mathbf{q} = \varepsilon_4\sigma\left(T_{amb}{}^4 - T^4\right)$ $\varepsilon_4 = 0.35$
B_5		$-\mathbf{n}\cdot\mathbf{q} = 0$
B_6		
B_7	$\mathbf{u}\cdot\mathbf{n} = u_{cast}$	$-\mathbf{n}\cdot\mathbf{q} = h_7\left(T_{amb} - T\right)$ $h_7 = 10$ W/(m²·K)

dence of losses from the surface of liquid titanium due to evaporation of $q_{ev}(T)$ is shown in Figure 2, *d* [9].

During calculations, as basic output data, the efficiency of ingot drawing (G = 250 kg/h) was taken, which corresponds to the basic speed of ingot drawing

$$u_{base} = \frac{4\cdot G}{\rho_{T_{out}}\cdot\pi\cdot d^2} = \frac{4\cdot 250}{4400\cdot\pi\cdot 0.4^2\cdot 3600} =$$

$$= 1.256\cdot 10^{-4}\ \text{m/s}\ (\text{approximately}\ 7.5\ \text{mm/min}),$$

the temperature of liquid metal at the inlet into the mould T_{in} = 2061 K and heating of the ingot is evenly distributed throughout the surface by a thermal flux of

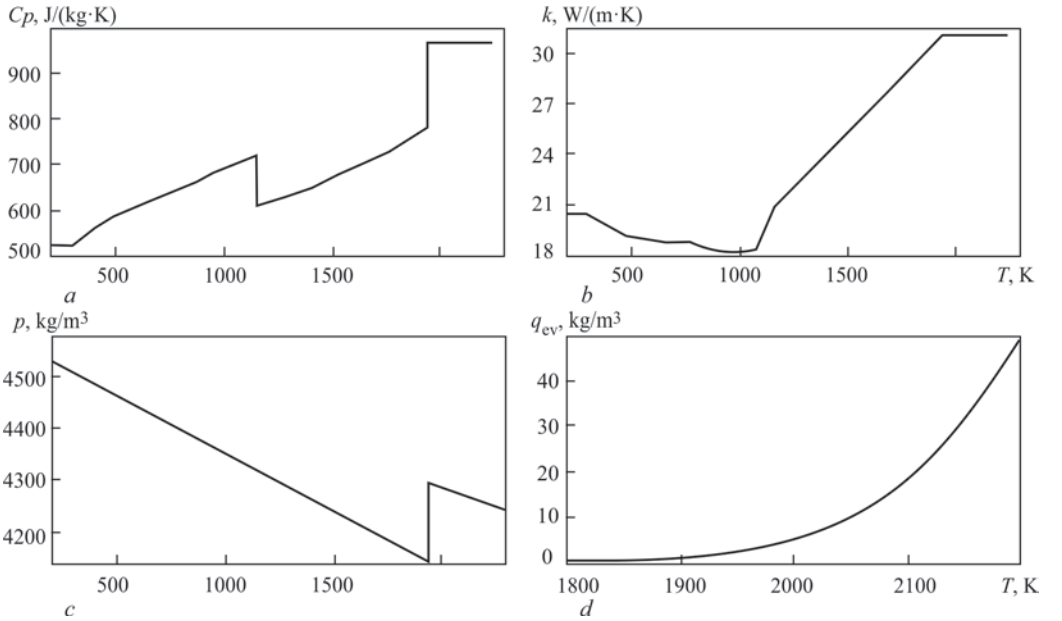

Figure 2. Dependences of specific heat capacity (*a*), coefficient of thermal conductivity (*b*), density (*c*) and evaporation (*d*) on temperature

a total power P_{eb} = 90 kW with an efficiency coefficient of electron beam heating being 75 %.

The importance and necessity of taking into account thermogravitation forces in the mathematical model of physical processes in the mould was determined and substantiated by comparing the results of calculations taking into account and without these forces. In order to study the degree of impact of the phenomenon of thermogravitation convection on the thermal state of the ingot and the position of the interphase boundary, the modeling of this process was carried out without taking into account the component ρ**g** in the equation (2). The temperature distribution, as well as the isotherms of solidus and liquidus (solid lines) are presented in Figure 3. In this case, the depth of liquid pool is 257 mm. For comparison, in Figure 3 the position of the interphase zone (dashing lines) is shown, obtained taking into account thermogravitation forces.

The results show that not taking into account thermogravitation forces leads to a more than twice increase in the depth of a liquid pool (by 137 mm) and, accordingly, to a change in the nature of the movement of liquid metal. In this case, shifting of the point of the maximum pool depth from the ingot axis is almost absent, despite the asymmetric view of the pool itself.

Therefore, the phenomenon of thermogravitation convection in the specified efficiency of EBM process is a significant factor that determines the thermal state of the ingot, so further calculations were performed, taking it into account.

To determine the exposure of the liquid metal to the overheating temperature, which is fed from the

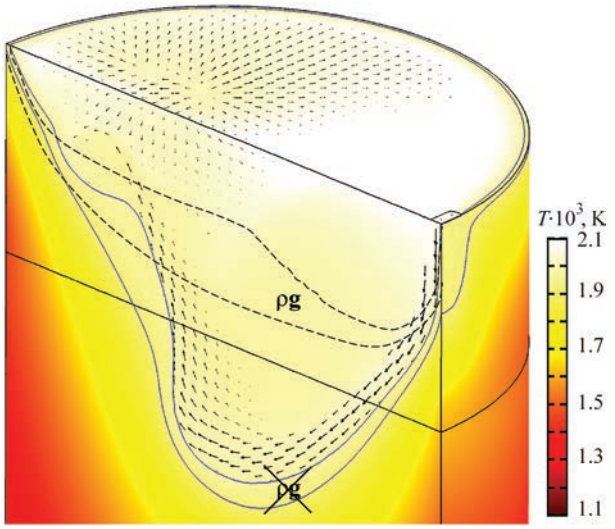

Figure 3. Impact of thermogravitation convection phenomenon on interphase zone position

cold hearth, calculations for different temperatures of the liquid metal at the inlet into the mould (T_{in}), K: 2041, 2061, 2081, 2101 were performed. As a result, in the studied zone distributions of temperature and speed were obtained, presented in Figures 4 and 5, respectively.

The analysis of distribution of temperatures in the ingot, obtained on the results of modeling showed that under the action of electron beam heating, the surface layer of a melt is heated to the maximum temperature — about 2085 K (Figure 4), which in some cases may even exceed the temperature of the liquid metal, that is fed from the cold hearth with a temperature of 2040–2100 K (Figure 4, *a*, *b*). Due to the intensive cooling of the liquid metal, the walls of the mould

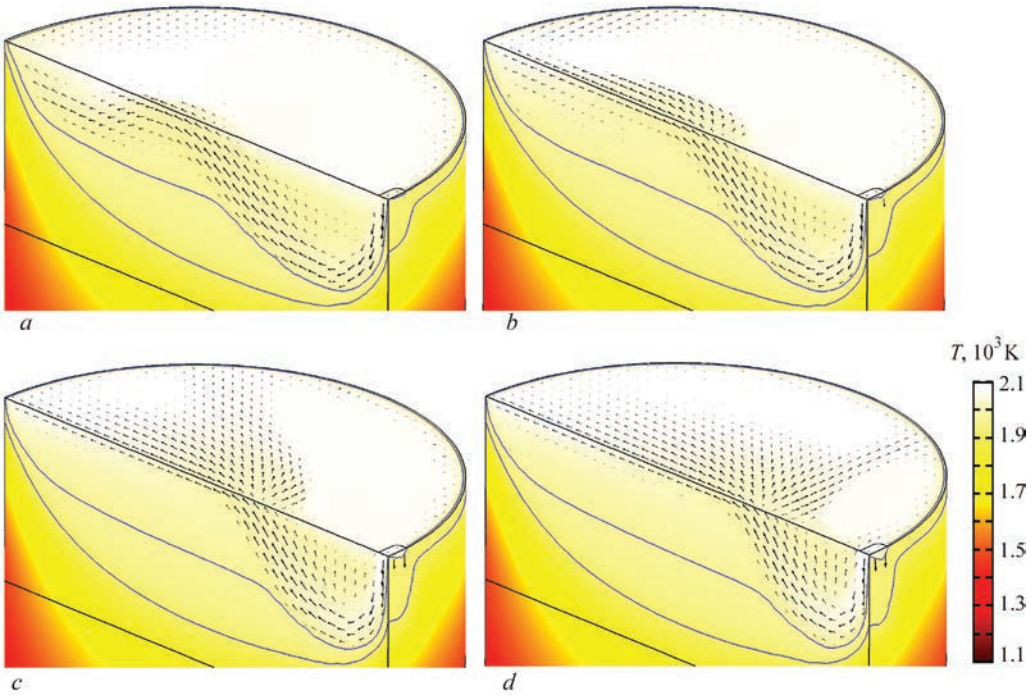

Figure 4. Distribution of temperature (T_{in}) in ingot during EBM, K: *a* — 2041; *b* — 2061; *c* — 2081; *d* — 2101

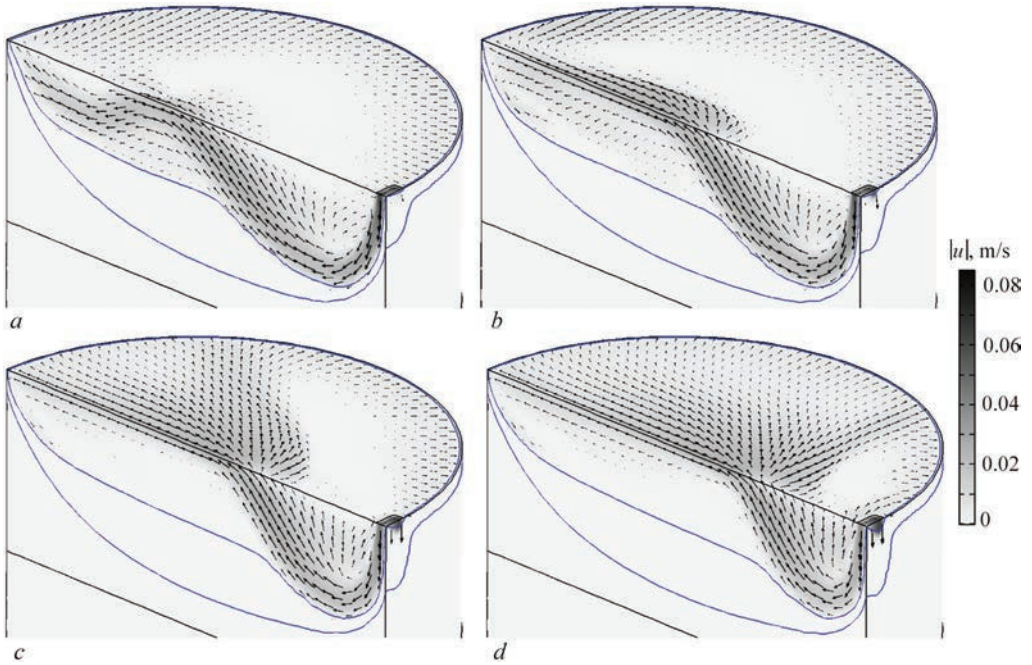

Figure 5. Distribution of melting speed (T_{in}) in ingot during EBM, depending on temperature, K: *a* — 2041; *b* — 2061; *c* — 2081; *d* — 2101

form the outer surface of the ingot in it, the thickness of the skull between the liquid metal and the wall of the mould in its upper part is 5–7 mm. Along the length of the ingot, the temperature decreases from 2085 K on the surface of a melt to 1000 K on its lower boundary of the calcualtion region. At the output of the ingot from the mould, the temperature of its surface is about 1500 K and weakly depends on the technological parameters of melting.

The analysis of the distribution of the rate of movement of the liquid metal in the mould showed that the flow of a melt from the cold hearth is deepened near the wall of the mould to the maximum depth and then mirrored from the bottom of the pool, gets to its surface and spreads throughout the volume of a melt (Figure 5, *a*, *b*). It should be noted that in the place of deepening of the inlet flow, the thickness of the two-phase zone is minimal and amounts to 3–6 mm. Under the conditions of a low overheating of a melt getting into the mould from the cold hearth, at the temperature, higher than the melting temperature of titanium, the movement of the liquid metal occupies the entire volume of the pool, where the temperature exceeds the liquidus temperature of titanium. Whereas with an increase in the temperature of the metal flow at the inlet, the melt movement is concentrated only near a free surface, forming quite volumetric stagnation zones (Figure 5, *c*, *d*). This phenomenon may be predetermined by the action of thermogravitation forces.

In general, the calculations showed that the shape of a liquid pool is asymmetric (Figures 4, 5). Although the crystallization front is approaching the plane one, in the region of the inlet zone of the liquid metal, washing of the solid phase near the wall of the mould is observed (Figure 6). The thickness of the skull in this zone is 2–3 mm, which is 2–3 times smaller than the thickness of the skull in other zones of the mould. During movement of the ingot downwards, such a thin skull can be destroyed and form well-known typical defects of metal tangling on the surface of the ingot.

Shifting of the maximum depth point relative to the ingot axis (d_{pool}) and the liquid pool depth (h_{pool}) depending on the overheating temperature on the liquid metal at the inlet into the mould are presented in Figure 7. These parameters were determined by the isotherm, which corresponds to the melting temperature of titanium (T_m = 1941 K).

It is interesting that with an increase in the metal temperature at the inlet into the mould (in the test range), shifitng of the point of the maximum pool depth from the ingot axis (Figure 7, *a*) decreases. Although it was expected, that with an increase in the overheating temperature of the liquid metal, fed from the cold hearth, the maximum liquid pool depth will be shifted from the ingot axis in the direction of the inlet of a liquid metal jet.

As for the depth of a liquid pool, it almost does not change in the test range of the temperature of the liquid metal at the inlet into the mould (Figure 7, *b*), based on which the conclusion can be made of their weak dependence. However, as can be seen from Figure 4, with an increase in the temperature of the liq-

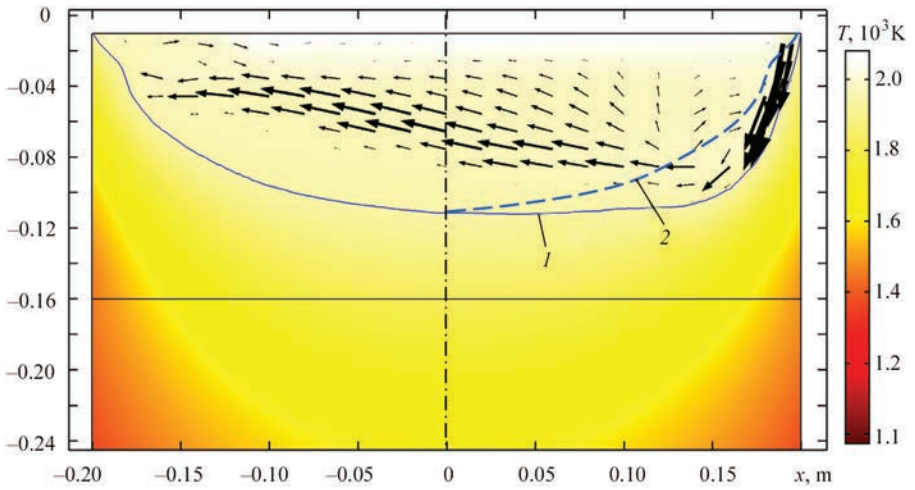

Figure 6. Longitudinal section of liquid pool in titanium ingot of 400 mm diameter during EBM; *1* —point of the maximum liquid pool depth; *2* — mirror projection of the left half of isotherm (T_m = 1941 K) relative to the ingot axis for visual evaluation of liquid pool asymmetry

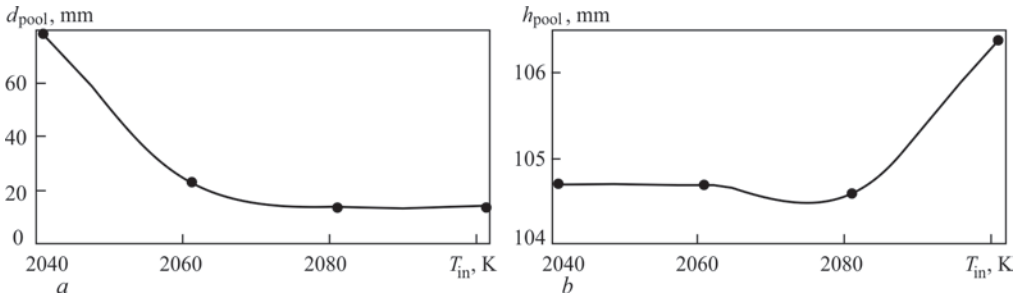

Figure 7. Dependences of shifting of the point of maximum depth relative to the ingot axis (*a*) and liquid pool depth (*b*) on overheating temperature of liquid metal at the inlet into the mould 8

uid metal at the inlet into the mould, the nature of its movement changes significantly.

While producing ingots by EBM method, one of the important technological parameters is the process efficiency. Therefore, further calculations were aimed at studying the impact of the feed rate of liquid metal from the cold hearth into the mould on the shape and depth of a liquid pool.

While modeling, the overheating temperature of the metal fed into the mould was taken as T_{in} = = 2061 K. The position of the isotherms, corresponding to the melting temperature of titanium (T_m) for different speeds of ingot drawing in the range of u_{cast}–$1.3u_{cast}$ are presented in Figure 8.

As is seen from Figure 8, with an increase in the efficiency of casting, configuration of the crystalli-

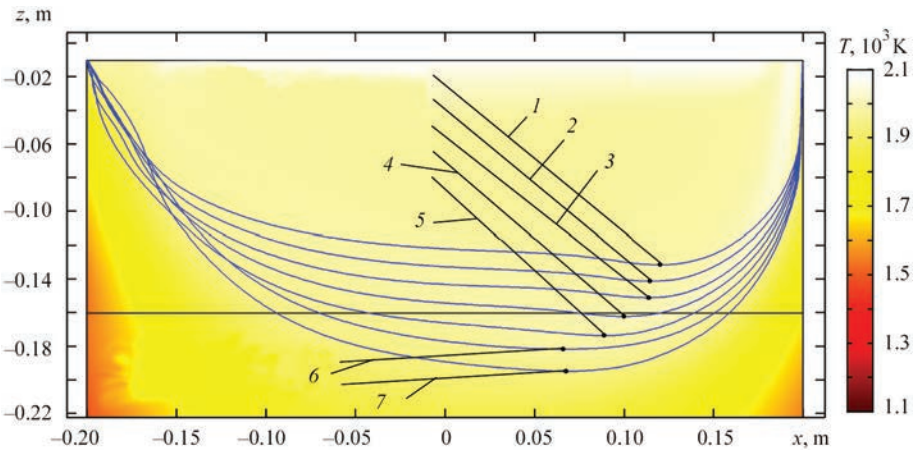

Figure 8. Position of isotherms of melting temperature of titanium for different speeds of ingot drawing from the mould (the point marks the place of the maximum liquid pool depth and its parameters are indicated in the format: u_{cast}; d_{pool}; h_{pool}, m): *1* — 1.00 u_{cast}; 0.120; 0.122; *2* — 1.05 u_{cast}; 0.116; 0.131; *3* — 1.10 u_{cast}; 0.114; 0.141; *4* — 1.15 u_{cast}; 0.100; 0.152; *5* — 1.20 u_{cast}; 0.088; 0.164; *6* — 1.25 u_{cast}; 0.066; 0.172; *7* — 1.30 u_{cast}; 0.068; 0.185

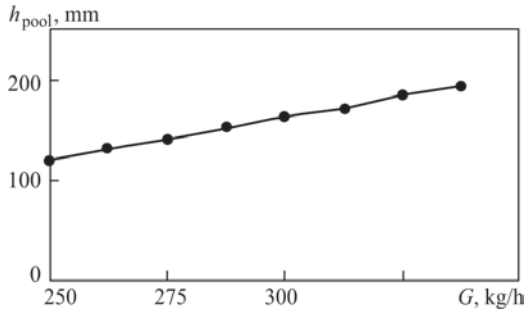

Figure 9. Dependence of liquid pool depth on efficiency during EBM of titanium ingot of 400 mm diameter

zation front, despite taking into account thermogravitation forces, is approaching to a cone-shaped one. This indicates that a more plane front of melt crystallization can be provided by reducing the efficiency of ingot casting. It is also clear that with a growth in efficiency, the impact of thermogravitation forces on the thermal state of the ingot will be weakened.

For a more clear demonstration of the results obtained with the help of a mathematical model of the carried out calculations, the dependence of the liquid pool depth on the efficiency of EBM process of titanium ingot was constructed (Figure 9).

As is seen from Figure 9, with an increase in the speed of ingot drawing by 30 %, the liquid pool depth increases by more than 50 % (from 0.122 to 0.185 m).

Analysis of the obtained results showed that a growth in the process efficiency, as in the case of increasing the overheating temperature of the metal getting into the mould, causes shifting of the maximum liquid pool depth point (d_{pool}) to the ingot axis. In addition, with a growth in the process efficiency, a significant increase in the liquid pool depth is observed, which is also confirmed by the data of [10].

Conclusions

1. Applying the methods of mathematical modeling of heat of mass transfer, the features of crystallization and metal pool configuration during EBM of titanium ingots in the mould of 400 mm diameter were established. Three-dimensional fields of speed of liquid metal movement and its temperature were obtained taking into account the action of thermogravitation forces for a laminar nature of melt movement.

2. The necessity of taking into account thermogravitation forces during modeling of hydrodynamic processes in the mould during EBM of titanium ingots was substantiated. It is shown that thermogravitation is a significant factor in determining the thermal state of the ingot, therefore, its consideration is mandatory. With the growth in EBM efficiency, the contribution of thermogravitation forces to the thermal state of the ingot will be weakened.

3. It was established that the impact of the overheating temperature of the liquid metal fed into the mould from the cold hearth on the configuration and depth of a liquid pool is insignificant. In the studied range of liquid metal temperatures at the inlet into the mould (2041–2101 K) with a change in temperature, the nature of its movement changes only slightly.

4. It was found that the impact of the efficiency of electron beam melting of titanium on the temperature distribution and, accordingly, on the shape and depth of a liquid pool is significant. With an increase in the speed of ingot drawing by 30 %, the depth of a liquid pool increases by 1.5 times (by 63 mm), and the point of the maximum liquid pool depth is approaching the ingot axis.

1. Bellot, J.-P., Flori, E., Ess, E., Ablizer, D. (1996) Mathematical modeling of electron beam melting process with cold hearth and its application for titanium manufacture. *Problemy Spets. Elektrometallurgii*, **4**, 27–37 [in Russian].
2. Paton, B.E., Trigub, N.P., Kozlitin, D.A. et al. (1997) *Electron beam melting*. Kiev, Naukova Dumka [in Russian].
3. Paton, B.E., Trigub, N.P., Akhonin, S.V., Zhuk, G.V. (2006) *Electron beam melting of titanium*. Kiev, Naukova Dumka [in Russian].
4. Lesnoj, A.B., Demchenko, V.F., Zhadkevich, M.L. (2001) Modeling of hydrodynamics and heat exchange in crystallization of ingots of electron beam remelting. *Problemy Spets. Elektrometallurgii,* **2,** 17–21 [in Russian].
5. Zhuk, G.V., Kalinyuk, A.N., Trigub, N.P. (2002) Modeling of conditions of removal of shrinkage pipe from cylindrical ingots. *Advances in Electrometallurgy*, **1**, 19–21.
6. Zhuk, G.V., Akhonina, L.V., Trigub, N.P. (1998) Mathematical modeling of crystallization processes of Ti–6Al–4V titanium alloy in EBCH. *Problemy Spets. Elektrometallurgii,* **2**, 21–25 [in Russian].
7. Akhonin, S.V., Gorislavets, Yu.M., Glukhenkiy, A.I. et al. (2019) Modeling hydrodynamic and thermal processes in the mould in cold-hearth electron beam melting. Suchasna Elektrometall., **4**, 9–17 [in Russian]. DOI: https://doi.org/10.15407/sem2019.04.02
8. Mills, K. (2002) *Recommended values of thermophysical properties for selected commercial alloys*. Woodhead publishing limited.
9. *Physical properties of titanium* [in Russian]. https:libmetal.ru/titan/phisproptitan.htm
10. Zhuk, G.V. (2008) On influence of metal heating power distribution in mould in EBCHM process on structure of titanium ingots. *Advances in Electrometallurgy*, **2**, 15–18.

Received 03.02.2021